Journal of Applied Electrochemistry (2005) 35:163–168
DOI 10.1007/s10800-004-6302-9

Improvement of electrochemical properties of PEO–LiTFSI electrolyte by incorporation of boroxine polymers with different backbone lengths

RUOYUAN TAO* and TATSUO FUJINAMI
*Department of Materials Science, Faculty of Engineering, Shizuoka University, Hamamatsu 432-8561, Japan (*author for correspondence, fax: +81-053-478-1162, e-mail: r5245008@ipc.shizuoka.ac.jp)*

Received 01 January 2004; accepted in revised form 12 October 2004

Key words: Boroxine ring, Discharge capacity, Interfacial resistance, Ionic conductivity, Lithium ion transference number

Abstract

A series of boroxine polymers (BP) with different backbone lengths were synthesized. Polymer electrolytes prepared by blending poly(ethylene oxide) (PEO) and BP with $Li(N(SO_2CF_3)_2)$ (LiTFSI) were evaluated. Better performance was observed by addition of BP in the PEO based polymer electrolyte. The effect of the backbone length of BP on electrochemical properties of PEO–BP–LiTFSI electrolyte systems was investigated. Compared with the PEO–LiTFSI system, about five times higher ionic conductivity at low temperature and five times higher lithium ion transference number at 70 °C were achieved by incorporation of long chain BP in the electrolyte. Short chain BP exhibited outstanding performance in decreasing interfacial resistances on both anode and cathode surfaces. Good battery performance was also observed for these BP containing hybrid polymer electrolytes.

1. Introduction

An impetus for research and development of solid polymer electrolytes has been the potential for making a safe lithium secondary battery [1]. Lithium ion conducting polymer electrolytes are considered as promising materials as safe alternatives to liquid electrolytes for application in high energy density electrochemical devices [2–6]. Since poly(ethylene oxide) (PEO) is subject to crystallization and lithium ion conduction takes place primarily in the amorphous phase [7–10], low ionic conductivity at ambient temperature and poor interfacial performance between the electrolyte and electrodes are observed for PEO-based electrolyte systems. Many efforts have been made to solve these problems such as introducing organic [11, 12] or inorganic plasticizers [13]. In our laboratory, a boroxine ring containing compound was synthesized. Although it exhibited good performance when blending with lithium salts [14, 15], low mechanic strength limited the application of such an electrolyte system.

PEO–$Li(N(SO_2CF_3)_2)$ (LiTFSI) polymer electrolyte system attracts much attention because of the high dissociating ability and plasticizing ability of LiTFSI and strong mechanic strength of the electrolyte film. However, low conductivity at ambient temperature and high interfacial resistance are still the problems for this electrolyte to be applied in lithium batteries. The purpose of this research is to develop a kind of third component to modify the PEO–LiTFSI system for better performance and explore the relationship between the composition of the third component and its effect on PEO–LiTFSI. We prepared a series of boroxine polymers (BP) with different backbone lengths and mixed them with PEO and LiTFSI to form hybrid polymer electrolytes. PEO–BP–LiTFSI electrolyte film is strong enough to separate the lithium anode from the cathode to avoid short circuit during cycling. The relationship between the composition of BP and the electrochemical properties of the polymer electrolyte is discussed.

2. Experimental

2.1. *Preparation of boroxine polymers (BP) and hybrid polymer electrolytes*

Poly(ethylene glycol) monomethyl ether (PEGMME 350, $CH_3O(CH_2CH_2O)_{7.2}H$) and tetraethyleneglycol (TEG), (Aldrich Chemical Co.), were dried by dry nitrogen bubbling under partial vacuum at room temperature for at least 24 h and were stored over molecular sieves prior to use. Poly(ethylene oxide) (PEO, Aldrich, Mw 5×10^6), lithium salts and all solvents were rigorously dried before use. Boric oxide (Merck) was used as supplied. Unless otherwise stated, all manipulations were carried out on a dry nitrogen/vacuum line or in an argon-filled glovebox for exclusion of moisture.

BP was prepared according to the method previously reported (Scheme 1) [14]. Boric oxide, PEGMME 350

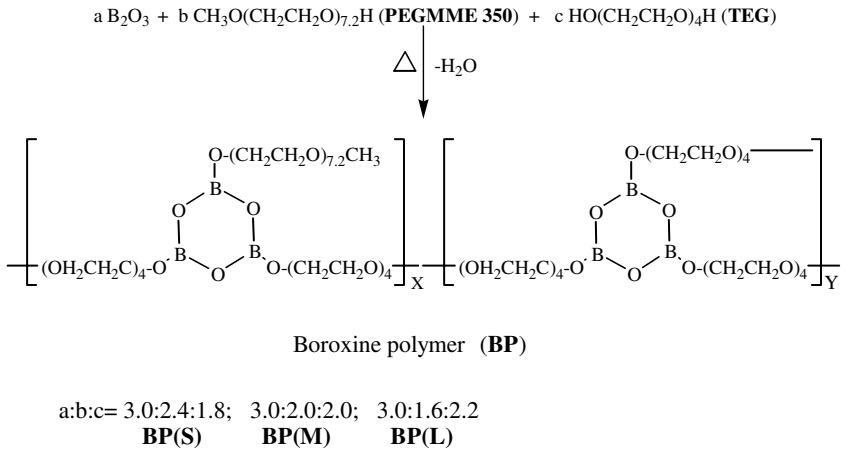

Scheme 1. Synthetic process for boroxine polymers (Bp(S): Short backbone length BP; BP(M): medium backbone length BP; BP(L): long backbone length BP).

and TEG were refluxed in toluene for 12 h using Dean–Stark apparatus for azeotropic removal of water produced. After removal of the solvent, BP was obtained. By changing the ratio of reagents, BP with different backbone lengths were synthesized. Here, three reaction ratios were applied: B_2O_3:PEGMME 350:TEG= 3.0:2.4:1.8, 3.0:2.0:2.0 and 3.0:1.6:2.2. In total, 3 kinds of BP, differing in the length of main chain, were prepared. They were denoted as BP(S), BP(M) and BP(L) respectively (S: short backbone length, M: medium backbone length, L: long backbone length). According to the literature [16, 17], the presence of a boroxine ring structure in synthesized BP ($\sim$719 cm^{-1}, B—O ring vibration; $\sim$1334 cm^{-1}, B—O ring stretching) and the absence of —OH were confirmed by IR spectroscopy.

Calculated amounts of BP, PEO and LiTFSI were dissolved in acetonitrile. After removal of the solvent, a solid hybrid polymer electrolyte was obtained. Unless otherwise stated, the ratios of EO unit (—CH_2CH_2O—) to Li^+ and PEO to BP in the electrolyte systems were fixed at 20:1 (by mole) and 9:1 (by weight), respectively.

2.2. *Preparation of cathode*

Calculated amounts of PEO and LiTFSI were dissolved in acetonitrile to obtain a homogeneous composite electrolyte. This works as a cathode binder. $LiCo_{0.2}Ni_{0.8}O_2$ and acetylene black were first ground in a mortar and then added slowly to the composite electrolyte solution. The mixture was vigorously stirred for 24 h and then treated with ultrasonic waves for 1 h. Part of the solvent was evaporated to give a slurry mixture. This composite cathode material was cast on aluminum substrates and dried under N_2 flow for 24 h. After being heated at 60 °C under vacuum for another 24 h, a black composite cathode was obtained. Before use, the cathode was pressed into a thin film. The composition of the composite cathode in weight ratio was strictly controlled as: $LiCo_{0.2}Ni_{0.8}O_2$:Composite electrolyte: acetylene black=65:20:15.

2.3. *Characterization*

IR spectra were recorded on a Jasco FT/IR-7000 IR spectrometer. The thermal behavior of polymer electrolytes was investigated using differential scanning calorimeter (DSC) (Perkin-Elmer Pyris 1 DSC). Samples were placed in aluminum pans and sealed under argon atmosphere. Heat-cool-reheat cycles were performed at a rate of 10 °C min^{-1}. All thermal events were obtained from the reheating cycle.

Ionic conductivities were determined by ac impedance measurement in the frequency range of 1 MHz to 1 Hz (signal amplitude 10 mV) using a Solartron 1260 frequency response analyzer and 1287 electrochemical interface. The thickness of the polymer electrolyte film sandwiched between blocking stainless steel electrodes was controlled using a Teflon spacer. The resistance (R_{int}) of the interface between the electrolyte and lithium or between the electrolyte and the cathode was determined using a similar process for samples sandwiched between non-blocking lithium electrodes or between composite cathodes. Lithium ion transference numbers (T^+) were determined for samples sandwiched between lithium electrodes using the combined ac impedance/dc polarization method of Evans et al. [18] modified by Abraham et al. [19]. The electrochemical stability window was determined by cyclic voltammetery of samples on a Pt working electrode and lithium reference and counter electrodes at a scan rate of 10 mV s^{-1} using a Solatron 1287 electrochemical interface. The cycling experiment was performed using a galvanostatic method at a cutoff voltage of 2.5–3.9 V at 70 °C. The current density was fixed at 0.2 mA cm^{-2}. The cell used for this study was assembled by sandwiching a polymer electrolyte film (about 200 μm) between a lithium foil anode and a composite cathode.

3. Results and discussion

Scheme 1 illustrates the process for BP preparation. Among the three reagents, PEGMME 350 with one —OH at one side of the EO chain was responsible for the formation of the side chain, while TEG with —OH at both sides and B_2O_3 formed the backbone of BP. Since all alcohols were reacted, which was confirmed by the absence of —OH in BP by IR spectra, increasing the quantity of TEG in the feed leading to the increase in BP chain length was assumed. Therefore, the sequence in backbone length of BP(S), BP(M) and BP(L) was suggested to be BP(S) < BP(M) < BP(L). Meanwhile, BP(S), BP(M) and BP(L) appear as viscous liquid, sticky soft solid and waxy solid, respectively at ambient temperature. According to the empirical relationship between the molecular weight and viscosity of polymers, $[\eta]=A[M]^{\alpha}$ (η: intrinsic viscosity, M: average molecular weight of a polymer, A and α: constants), the above described sequence in backbone lengths of BP was confirmed.

Thermal events obtained from DSC measurement during the reheating cycle can be seen in Table 1. An endothermic peak (T_m) was observed around 63.3 °C for the PEO–LiTFSI electrolyte system and the crystallinity (χ) of PEO evaluated by enthalpy of fusion (ΔH) was calculated to be 0.59. Incorporation of BP in PEO–LiTFSI decreased T_m and χ. Thus, the proportion of amorphous phase in the electrolyte was increased. Furthermore, long chain BP being more effective in decreasing T_m and suppressing crystallization of PEO was also observed while blending with PEO–LiTFSI. This was ascribed to the fact that long chain BP is easier to entangle with the PEO chain due to its long backbone; thus more defects in PEO are formed and the crystallization process is further hindered, leading to lower T_m and χ.

The temperature dependence of the ionic conductivities of PEO–BP–LiTFSI electrolytes is illustrated in Figure 1. PEO–LiTFSI was introduced as a reference system. A sharp drop on conductivity in the temperature region of 65–60 °C was observed for the PEO–LiTFSI electrolyte. It was related to the crystallization of PEO. However, for other electrolytes with the presence of BP, the sharp drop was pushed to lower temperatures. This result concurs with T_m data obtained from DSC measurement. At low temperature, BP containing systems exhibited higher ionic conductivities than the pure PEO system. With increase in BP chain length, an enhancement of ionic conductivity was observed in PEO–BP–LiTFSI electrolytes. BP(L) and BP(M) showed better performance than BP(S) in improvement of conductivity. This is due to the fact that lithium ion transference primarily takes place in the amorphous phase in the PEO system. Long backbone BP is more effective in suppressing PEO crystallization and a larger proportion of amorphous phase results, as shown by χ values obtained from DSC measurement. Therefore, a larger number of ions can be transported in long chain BP containing electrolyte.

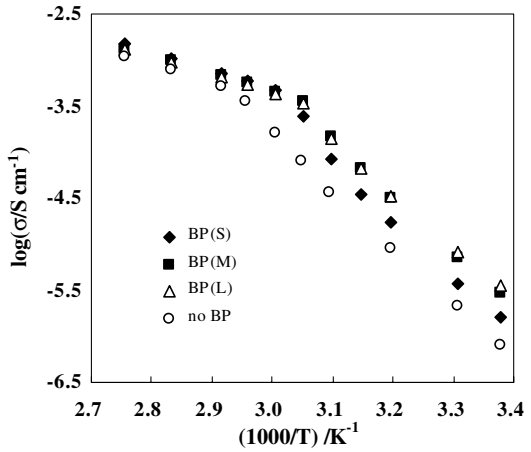

Fig. 1. Ionic conductivities of PEO–BP–LiTFSI and PEO–LiTFSI electrolyte systems. EO:Li^+ = 20:1, PEO:BP = 9:1.

High lithium ion transference number (T^+) is an important factor for quick charge–discharge, large current lithium battery. BP can entangle with the PEO chain or itself and the boroxine ring containing BP can trap anions of lithium salts due to its electron deficient property [16, 17]. The mobility of the BP–anion complex should be lower than that of the free anion because of the larger volume of the BP–anion complex. Thus, an improvement in T^+ relating to BP chain length is apparent. The results shown as the dependence of T^+ on BP structures in PEO–BP–LiTFSI electrolytes are presented in Table 2. At 70 °C, the PEO–LiTFSI electrolyte system gave a T^+ of 0.05, while PEO–BP(L)–LiTFSI showed a T^+ value of 0.23. This is about five times higher than that of the pure PEO system. An increase in T^+ can be obviously seen with the increase in BP chain length. Compared with PEO–BP(S)–LiTFSI, PEO–BP(L)–LiTFSI exhibited about three times higher T^+ at 70 °C. The dependence of the mobility of the

Table 1. Thermal characteristics of polymer electrolytes

Electrolytes*	T_m/°C	$\Delta H/W$/J g^{-1}	Crystallinity (χ)
PEO–LiTFSI	63.3	125.7	0.59
PEO–BP(S)–LiTFSI	58.2	100.9	0.47
PEO–BP(M)–LiTFSI	57.6	96.4	0.45
PEO–BP(L)–LiTFSI	57.4	94.4	0.44

*EO:Li^+ = 20:1; PEO:BP = 9:1.

Table 2. T^+ of PEO–BP–LiTFSI electrolytes at 70 °C

Electrolytes*	Lithium ion transference number (T^+)
PEO–LiTFSI	0.05
PEO–BP(S)–LiTFSI	0.08
PEO–BP(M)–LiTFSI	0.14
PEO–BP(L)–LiTFSI	0.23

*EO:Li^+ = 20:1; PEO:BP = 9:1.

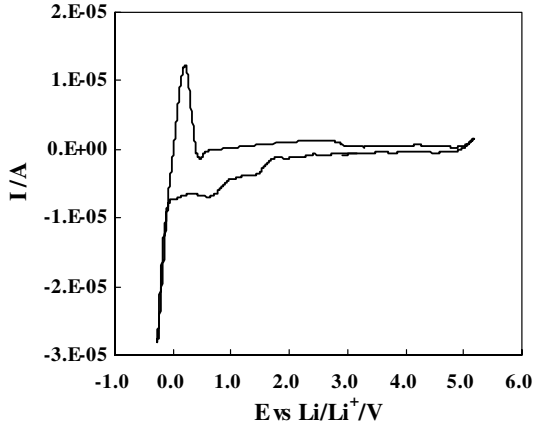

Fig. 2. Cyclic voltammetery of PEO–BP(S)–LiTFSI at a scan rate of 10 mV s^{-1} at 60 °C. Working electrode: Pt; Counter and reference electrodes: Li. Electrode area: 0.16 cm^2.

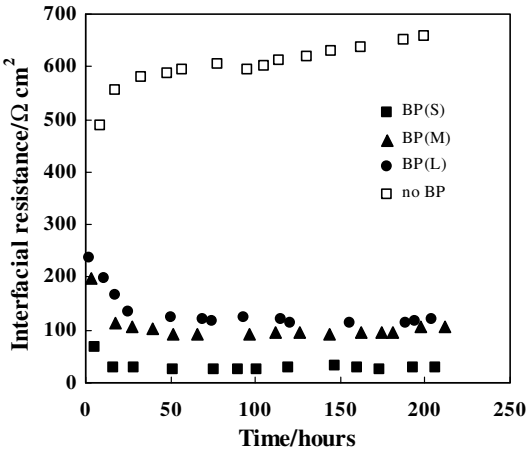

Fig. 3. Time dependence of interfacial resistances of PEO–BP–LiTFSI electrolytes/lithium metal at 70 °C. EO:Li^+ = 20:1; PEO:BP = 9:1.

BP–anion complex on the BP backbone length accounts for this result.

The electrochemical stability window is another important factor for the polymer electrolyte. A wide range of electrochemical stability window allows the lithium battery a large choice of redox couples as electrode materials [20]. Figure 2 shows the cyclic voltammetery of the PEO–BP(S)–LiTFSI electrolyte obtained at a scan rate of 10 mV s^{-1}. The electrochemical stability window was estimated to be 4.8 V vs Li/Li^+. We also determined the stability windows of PEO–LiTFSI and PEO–BP(L)–LiTFSI to be about 4.7 V vs Li/Li^+. These results indicated that addition of BP in PEO–LiTFSI has no deleterious effect on the electrochemical stability of the electrolyte.

The electrode/electrolyte interface plays an important role for long life lithium batteries. Due to complex reactions between the electrolyte and the electrode, a low conductivity layer may be formed at the electrode surface. Increase in interfacial resistance (R_{int}) during charge-discharge of cells is often observed. In some cases, R_{int} is more than 10 times higher than the bulk resistance of the electrolyte. This may be a major reason for the power fade of the cell [21]. How to improve the compatibility between the electrolyte and the electrode is a major subject for polymer electrolyte research. The results of the influence of BP with different backbone lengths on the PEO–BP–LiTFSI electrolyte/lithium interface are illustrated in Figure 3. R_{int} of BP containing electrolytes at the surface of lithium metal are much lower and more stable than that of PEO–LiTFSI electrolyte. It was reported [22] that, in a liquid electrolyte, when the boric ester contacts lithium metal, a protective single ion conduction film composed of amorphous $LiBO_2$ may be formed. This film is effective in stabilizing the electrolyte/lithium interface and decreasing R_{int}. Since BP is also a kind of boric ester, it is believed that the effect of BP on stabilizing and decreasing R_{int} is related to the formation of a $LiBO_2$ layer on the lithium surface. At 70 °C, R_{int} of PEO–LiTFSI/Li was determined to be around 600 Ω cm^2; whereas PEO–BP(L)–LiTFSI, PEO–BP(M)–LiTFSI and PEO–BP(S)–LiTFSI systems exhibited a R_{int} of about 120, 100 and 30 Ω cm^2, respectively. Short chain BP leading to better interfacial performance was obviously seen. Steric effect accounts for this phenomenon. Compared with long chain BP, short chain BP is easier to move to the interface and have better contact with lithium metal, resulting in the formation of a denser $LiBO_2$ film responsible for lower R_{int}. In addition, short chain BP which makes the polymer electrolyte softer, gives better contact with lithium metal and may also partially contribute to the decrease in R_{int}.

In a lithium battery, besides the interface between the electrolyte and the lithium anode, another interface between the electrolyte and the cathode should also be considered because the high resistance film formed by the reaction between the electrolyte and the active material in the cathode will cause a loss of the capacity of the cell during cycling. However, this interface has not been widely studied. Using a widely used active material, $LiCo_{0.2}Ni_{0.8}O_2$, a composite cathode was prepared. The effect of BP with different backbone lengths on PEO–BP–LiTFSI/composite cathodes interface was studied. The results shown as the time dependence of R_{int} are illustrated in Figure 4. At 70 °C, R_{int} of the PEO–LiTFSI/cathode interface increased significantly from 160 Ω cm^2 in the fresh cell to 260 Ω cm^2 after 200 h of testing due to the formation and thickening of the low conductivity passivation layer at the surface. As to BP containing systems, much lower and more stable R_{int} were clearly seen. R_{int} of PEO–BP(L)–LiTFSI and PEO–BP(S)–LiTFSI systems were determined to be about 100 Ω cm^2 and 40 Ω cm^2, respectively and remained almost constant with the progress of testing. The reason for such an effect of BP is suggested to be that, when BP contacts cathode particles, it suppresses the formation of the low conductivity layer and forms a stable, low resistance film for lithium

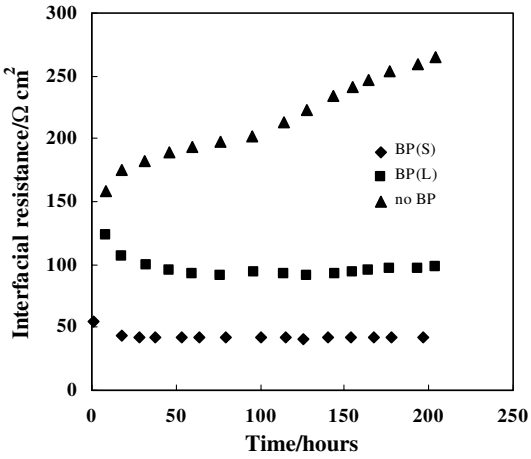

Fig. 4. Time dependence of interfacial resistances of PEO–BP–LiTFSI electrolytes/composite cathode at 70 °C. EO:Li^+ = 20:1; PEO:BP = 9:1.

ion transference like the $LiBO_2$ amorphous film formed at the lithium metal surface. Compared with long chain BP, short chain BP exhibited better performance in decreasing R_{int}. This may also be ascribed to the higher mobility of short chain BP and easier contact with composite cathode particles.

As polymer electrolytes are designed for application in lithium batteries, the best way to estimate their performance is to do battery testing. In this work, $LiCo_{0.2}Ni_{0.8}O_2$ was selected as the active material in composite cathodes due to its high specific capacity and low cost [23]. Figure 5 shows the charge–discharge results of Li/Polymer electrolyte/$LiCo_{0.2}Ni_{0.8}O_2$ cells at a current density of 0.2 mA cm^{-2} at a cutoff voltage of 2.5–3.9 V at 70 °C. A significant capacity fade was observerd for the Li/PEO–LiTFSI/$LiCo_{0.2}Ni_{0.8}O_2$ cell. The discharge capacity declined from 95 mAh g^{-1} in the fresh cell to 71 mAh g^{-1} after 50 cycles (~25 percent power in loss). Whereas, no significant capacity fade was observed for BP containing cells. Only about 6% of the capacity was lost after 50 cycles of testing for Li/PEO–BP(S)–LiTFSI/$LiCo_{0.2}Ni_{0.8}O_2$ cell. This is ascribed to the different conditions of R_{int} of the interfaces between the electrolyte and electrodes in these cells. As to the PEO–LiTFSI system, the capacity fade upon cycling can be explained by the rapid increase in interfacial resistance. Addition of BP in PEO–LiTFSI leads to stable interfaces. Therefore, no significant power loss is observed. As shown in Figure 5, the short chain BP (BP(S)) based cell exhibited higher discharge capacity (~112 mAh g^{-1}) than the long chain BP (BP(L)) based cell and the cell containing no BP. This was also related with the cell resistance. As all the polymer electrolytes show similar bulk resistance at 70 °C (Figure 1), lower voltage drop due to cell resistance is expected in BP(S) containing cells because of the low R_{int}, which results in higher discharge capacity.

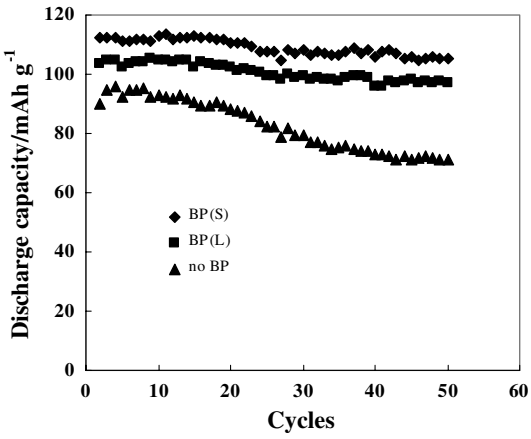

Fig. 5. Discharge capacity of Li/Polymer electrolyte/$LiCo_{0.2}Ni_{0.8}O_2$ at a cutoff voltage of 2.5–3.9 V at 70 °C. Current density: 0.2 mA cm^{-2}.

4. Conclusion

Using different ratios of reagents, several kinds of BP were prepared. Incorporation of BP in the PEO–LiTFSI electrolyte leads to positive effects on ionic conductivity, lithium ion transference number and interfacial performance. With increase in BP backbone length, higher ionic conductivity at low temperature and higher lithium ion transference number were obtained in PEO–BP–LiTFSI electrolytes. Short chain BP is greatly favored in decreasing interfacial resistances at the surfaces of both the lithium anode and the composite cathode. Capacity fade is depressed by the introduction of BP into the PEO–LiTFSI electrolyte. The Li/PEO–BP(S)–LiTFSI/$LiCo_{0.2}Ni_{0.8}O_2$ cell exhibits higher discharge capacity than the corresponding BP(L) or no BP containing cells.

Acknowledgements

The authors are grateful to Genesis of Research Institute Inc. for financial support.

References

1. J.R. Maccallum and C.A. Vincent, *Polymer Electrolyte Reviews*, Vol. 1 (Elsevier Applied Science Publishers, London and New York, 1987), p. 351.
2. H.R. Allcock, S.E. Kuharcik, C.S. Reed and M.E. Napierala, *Macromolecules* **29** (1996) 3384.
3. Y. Tominaga and H. Ohno, *Solid State Ionics* **124** (1999) 323.
4. M. Watanabe, T. Endo, A. Nishimoto, K. Miurs and M. Yanagida, *J. Power Sources* **81–82** (1999) 786.
5. G.B. Appetecchi, G. Dautzenberg and B. Scrosati, *J. Electrochem. Soc.* **143** (1996) 6.
6. M. Forsyth, D.R. MacFarlane, A. Bes, J. Adebahr, P. Jacobsson and A.J. Hill, *Solid State Ionics* **147** (2002) 203.
7. C.C. Lee and P.V. Wright, *Polymer* **23** (1982) 681.
8. D.R. Payne and P.V. Wright, *Polymer* **23** (1982) 690.
9. J.E. Weston and B.C.H. Steele, *Solid State Ionics* **7** (1982) 75.
10. R. Dupon, B.L. Papke, M.A. Ratner, D.H. Whitmore and D.F. Shriver, *J. Am. Chem. Soc.* **104** (1982) 6247.

11. S. Chintapalli and R. Fresh, *Solid State Ionics* **86–88** (1996) 341.
12. L.R.A.K. Bandara, M.A.K.L. Dissanayake and B.-E. Mellander, *Electrochim. Acta* **43** (1998) 1447.
13. B. Kumar and L.G. Scanlon, *J. Power Sources* **52** (1994) 261.
14. M.A. Mehta and T. Fujinami, *Solid State Ionics* **113–115** (1998) 187.
15. M.A. Mehta, T. Fujinami, S. Inoue, K. Matsushita, T. Miwa and T. Inoue, *Electrochim. Acta* **45** (2000) 1175.
16. M.F. Lappert, *J. Chem. Soc.* (1958) 2790.
17. F.A. Grimm, L. Barton and R.F. Porter, *Inorg. Chem.* **7** (1968) 1309.
18. J. Evans, C.A. Vincent and P.G. Bruce, *Polymer* **28** (1987) 2324.
19. K.M. Abraham, Z. Jiang and B. Carroll, *Chem. Mater.* **9** (1997) 1978.
20. M.C. Borghini, M. Mastragostino, S. Passerini and B. Scrosati, *J. Electrochem. Soc.* **142** (1995) 2118.
21. K. Amine, C.H. Chen, J. Liu, M. Hammond, A. Jansen, D. Dees, I. Bloom, D. Vissers and G. Henriksen, *J. Power Sources* **97–98** (2001) 684.
22. S.S. Zhang and C.A. Angell, *J. Electrochem. Soc.* **143** (1996) 4047.
23. C. Delmas, I. Saadoune and A. Rougier, *J. Power Sources* **44** (1993) 595.